Max McIntyre

Electric field effect on the magnetism of $(La_{0.4}Pr_{0.6})_{0.67}Ca_{0.33}MnO_3$

I. Introduction

Perovskite manganese-oxides (manganites) have shown complex behaviors such as colossal magnetoresistance (CMR) and colossal electroresistance (CER). These effects are based on small changes in externally applied magnetic or electric fields that then cause larger changes in the resistance of the manganite. [1] [2] Manganite thin films, such as $(La_{1-y}Pr_y)_{1-x}Ca_xMnO_3$ (LPCMO), can form multiphase regions at low temperatures. The afore mentioned effects can arise due to a phase competition of ferromagnetic metallic (FMM) and antiferromagnetic charge-ordered insulator (AFM-COI) regions. [3] Controlling the FMM regions using external fields will provide a greater understanding of the effects of phase competition on the physical properties of materials. These properties could then lead to applications such as bolometers and cryogenic memories. [4] [5]

It is largely accepted that phase competition exists on the scale of nanometers to micrometers. Studies have shown that by reducing the manganites physical dimensions to that at which the phase competition occurs, the magnetic behavior is changed, then affecting properties such as the coercive field and anisotropy constants. [6] [7] By creating microstructures of manganite thin films; we can control coercive fields, leading to a greater understanding of magnetic interactions. However, this ability is limited by the magnitude of the applied electric field which in turn is limited by the dimensions of the contact array. In our experiment, we attempt to create microstructure contact arrays that increase the applied electric field. To create an electrical contact, gold is chosen as it is a good conductor and can be easily deposited by sputter deposition. Therefore our experiment assesses the capability of gold microstructures to form a contact with the LPCMO thin films and optimizing their fabrication process. Here, we

report that Au thin film contacts can replace soldered In pads. The fabrication process for creating the microstructure contacts has been determined to require an image reversal liftoff. By comparing a pre and post-photolithography LPCMO thin film, our data shows that microstructured LPCMO has an increased coercive field. The fabrication of a gold microstructure contact arrays needs to be optimized so that a complete pattern transfer occurs.

II. Experimental Details

A. Gold vs. Indium Contact Study

Two $(La_{1-y}Pr_y)_{1-x}Ca_xMnO_3$ thin films on NGO substrate were used to test the type of contact gold formed versus the traditional soldered indium contact. In previous experiments, gold wires were soldered to the LPCMO samples with indium. This standard procedure was carried out on one of the LPCMO films [Fig. 1(a)]. The other film had 20nm of titanium and 100nm of gold deposited via sputter deposition. Gold wires were then bonded to the gold thin film with silver paste [Fig. 1(b)]. The contacts were compared through current-voltage characteristics at room temperature and 20K. Both samples were attached with GE varnish to a sapphire substrate then the gold wires were soldered to copper wires that were connected to a four-pin connector. The sample was then inserted into the circuit in Fig. 1(c). In this circuit, the voltage drop across the standard resistor R=100 kΩ was measured with a voltmeter. From this measurement, V_R/R was the current in the circuit was and $V_S=V_O-V_R$ was the voltage. Plotting current vs. voltage, the slope then represents the resistance of the sample, $R_S=(V_O-V_R)\cdot(R/V_R)$. While running the measurement, the V_O was varied. These characteristics were checked at room temperature and at 20K. [1]

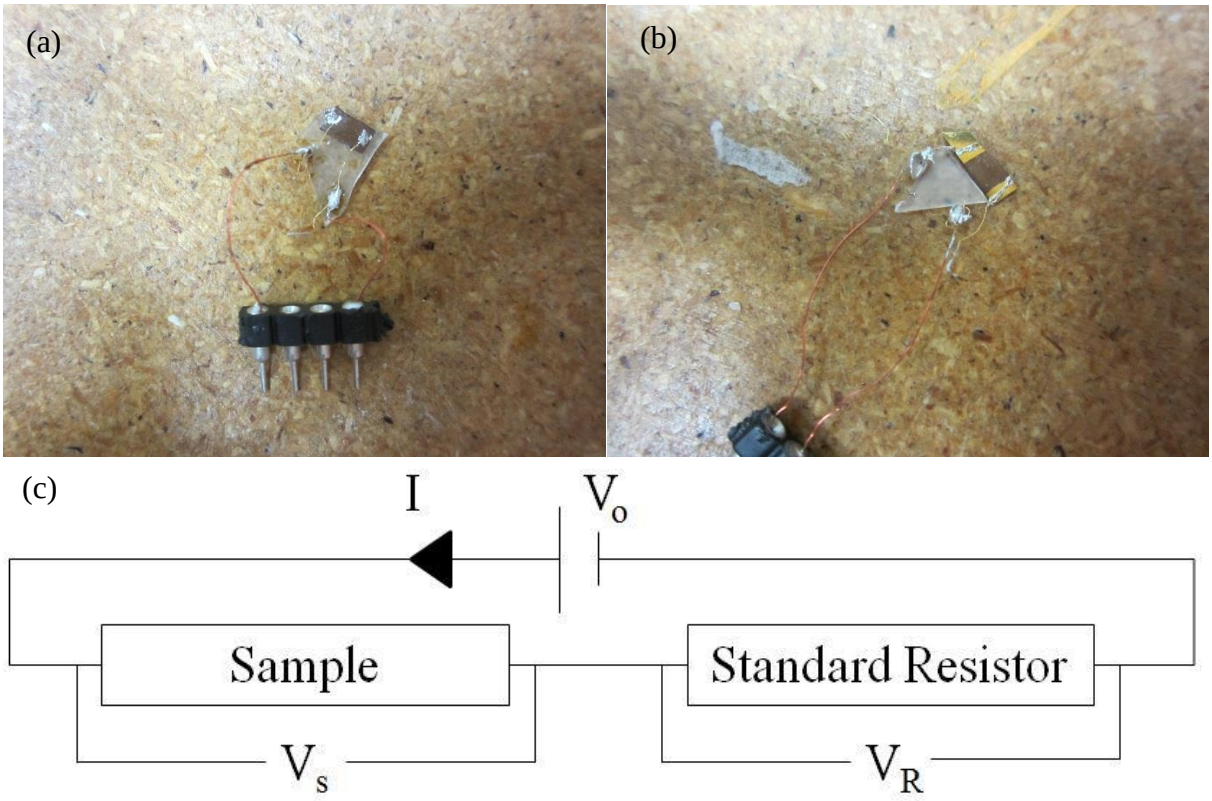

Figure 1: (a) Indium contact with soldered gold wires on LPCMO thin film. (b) Gold contact with gold wires bonded by silver paste on LPCMO thin film. (c) Schematic of the circuit created to perform IV measurements.

B. LPCMO Thin Film and Gold Contact Microstructuring

A $(La_{0.4}Pr_{0.6})_{0.67}Ca_{0.33}MnO_3$ (LPCMO) thin film was grown by pulsed laser deposition (PLD) on a 5 x 5mm (110) $NdGaO_3$ (NGO) substrate. The sample was oriented so that the easy axis would align with the magnetic field [Fig. 2(d)]. Before being patterned, the magnetic properties of the film were measured using a Quantum Design 5T superconducting quantum interference device (SQUID) magnetometer. A degaussing sequence was run at 150K (above the materials Curie temperature) before each measurement. This was necessary because LPCMO thin films have thermal and magnetic hysteresis. Magnetization vs. applied magnetic field measurements were done at temperatures from 10-100K. For each measurement the applied field was raised to +/-5000 Oe and scanned more precisely by 50 Oe steps between +/-800 Oe. The raw magnetization data from the SQUID has signals from both the ferromagnetic LPCMO film and the paramagnetic NGO substrate. To find the ferromagnetic signal, a linear fit of the raw data greater than the coercive field was made. [7] This function signifies the paramagnets magnetic moment and can then be subtracted from the raw data leaving the LPCMO films magnetic moments.

The sample was then put through a photolithography process to alter the manganite pattern. To do so, a photomask was created using the program Layout Editor. With this program the clear areas of the photomask can be drawn. For most designs it is best to draw the desired pattern, then invert if necessary. For this sample, a 27 x 27 array of 100μm squares separated by 10μm was created on the photomask. Alignment markers were added to either outer edge of the design [Fig. 2(a)]. This design was then inverted by the mask writer to create the iron oxide interference pattern instead of the clear glass. The sample was coated in positive photoresist, AZ 1512, to a thickness of .8μm using a Suss Delta 80 spinner. The sample was then baked in an

oven at 105°C to remove solvents in the photoresist. Then using a Karl Suss MA6 mask aligner, the pattern of the photomask was aligned with the sample. Then the sample was exposed to an ultraviolet lamp of intensity 8.0W/m^2 for a duration of 40 seconds. The sample was then put in a bath of AZ 300 MiF developer for 40 seconds. This developer washes away any photoresist that was exposed to the UV light, therefore leaving a square array of photoresist. Then using an etchant composed of H_20 + KI + 10% HCL, the LPCMO film was etched where the photoresist did not remain. Then the remaining photoresist was removed by sonicating in acetone and ethanol. The removal of the LPCMO was confirmed by reading a short with a multimeter. The LPCMO square array was confirmed by optical microscope.

Following the patterning of LPCMO, the sample was placed in the SQUID magnetometer. The process was the same as the previous SQUID measurements except only the temperatures 10K, 40K, 45K, 50K, and 60K were measured. This was done to investigate the effects patterning has on the single to multi-domain transition and the coercive field. An AFM scan was run to confirm the thickness of the LPCMO thin film and dimensions of the pattern.

A second photomask was developed for the purpose of creating microstructure contact arrays. The contact array was made of 10μm wide contact strips that run parallel over two edges of each square. The strips then connect to 500μm square contact pads in each corner [Fig. 2(c)]. To achieve this contact array a liftoff process using an image reversal bake was necessary. Therefore the design of the photomask in Layout Editor must be inverted by the mask writer so that the patterns are dark. To begin the liftoff process, the pattern LPCMO sample was coated with AZ 1512 positive photoresist to a thickness of 1.3μm using a Suss Delta 80 spinner, then baked at 105°C for 25 minutes. The sample was taken to the mask aligner where the alignment marks from the first photolithography pattern were aligned with the marks on the second

photomask [Fig. 2(c)]. The sample was exposed to UV light for 40 seconds by a 400W Mg lamp of intensity 8.0W/m^2. The sample was then placed in the YES oven for image reversal for 90 minutes. The oven uses ammonia to reverse the tone of positive photoresist. Then it was flood exposed to UV light for 60 seconds using the mask aligner. A 4:1 ratio of DI water to AZ 400K developer was used for 1 minute to wash away the soluble resist. Before depositing the contacts, the surface of the film was descummed, removing photoresist and developer residues. For this, an Anatech Barrel SCE600 asher was used at 400W power supply and 600 sccm of O_2 for 2 minutes. A Kurt J. Lesker Multi-Source RF and DC Sputter System was used to deposit a 20nm adhesion layer of titanium and a 100nm contact layer of gold. The process was completed by sonicating the sample in acetone to remove the photoresist and the gold on top.

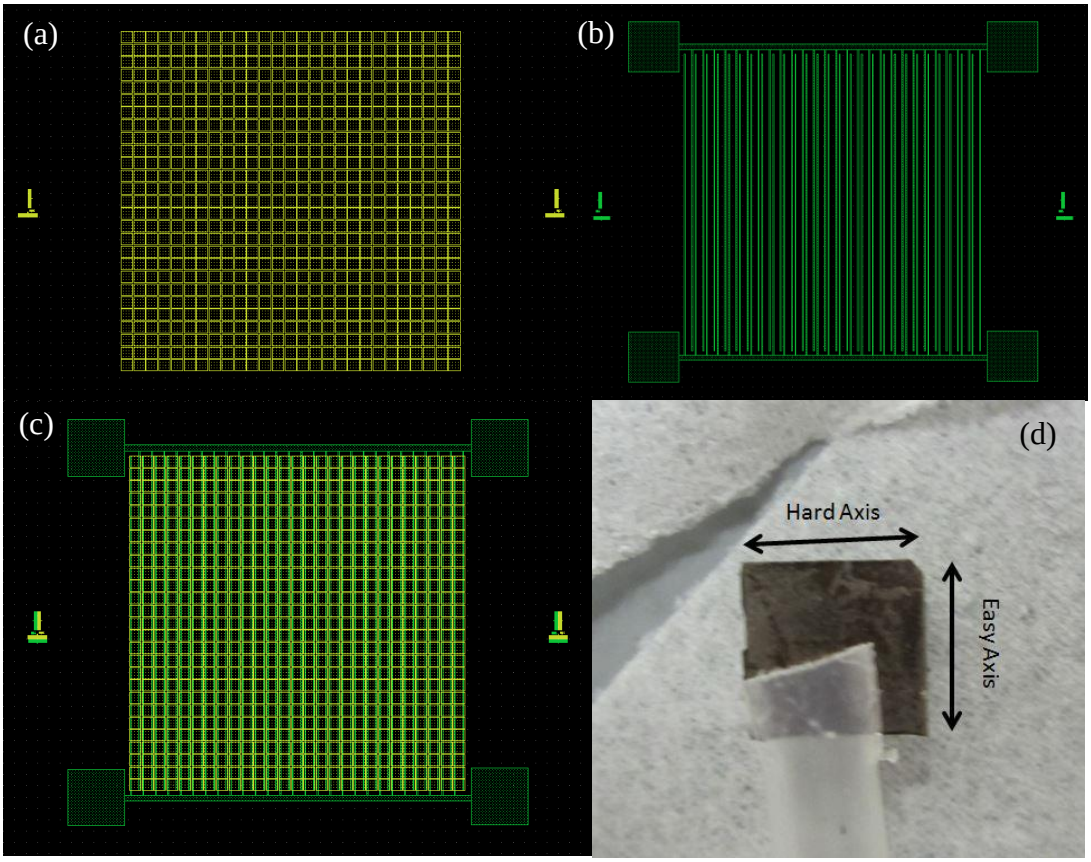

Figure 2: (a) 27 x 27 array of 100µm squares with 10µm separation. This pattern is used for the initial manganite etch back procedure. (b) 500µm square contact pads with 10µm wide contact strips. This pattern is used to the gold contact liftoff process. (c) The two previous layers aligned using the 10X magnification alignment marks on the left and right. (d) LPCMO thin film sample before placing into SQUID magnetometer, also illustrating the hard and easy axes.

III. Results and Discussion

A. Contact IV Characteristics

Fig. 3 shows the IV curves of LPCMO thin films with either Au thin film contacts or soldered In pads at room temperature (a) and 20K (b). The room temperature IV curve in Fig. 3(a) shows a linear relationship between current and voltage. This indicates that both Au and In form an ohmic contact with the LPCMO, meaning there is a low resistance junction between the materials. Differing IV slopes point to the samples having changed resistance, most likely during the low temperature measurements. The 20K IV curve in Fig. 3(b) shows a non-linear relationship between current and voltage for both contacts. This means the contacts are non-ohmic, although this is likely due to the sample. By showing the similarities in the IV curves between Au and In, the use of gold thin film microstructures as contacts is confirmed as a viable option.

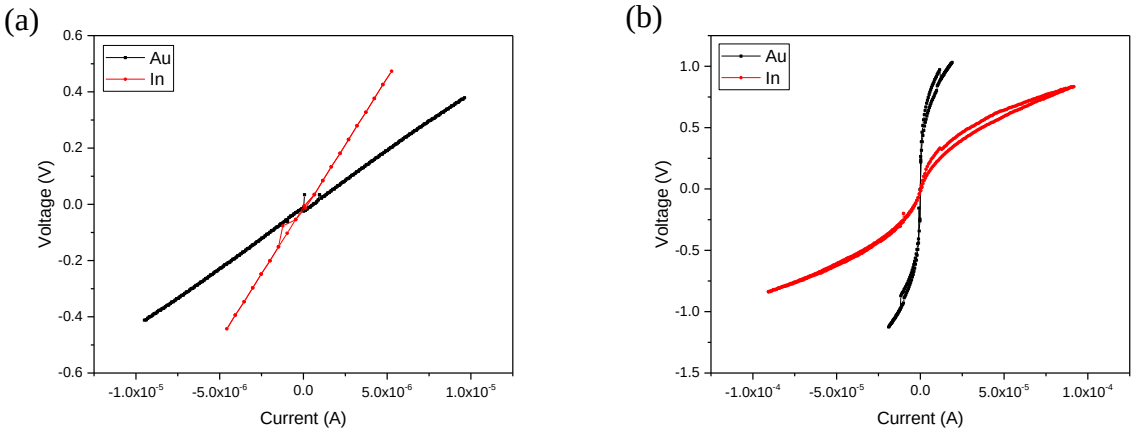

Figure 3: (a) IV characteristic for Au and In at room temperature. (b) IV characteristic for Au and In at 20K.

B. Effects of Microstructuring LPCMO Thin Films using Photolithography and Liftoff

The etch back procedure of patterning the LPCMO thin film with an array of 100μm squares is an optimized process stemming from former researchers work. This pattern transfer therefore is accurate and all the LPCMO outside the squares is removed as seen in Fig. 4(a). By forming these microscale squares, the patterns scale matches the phase coexistence scale. The dipole moments of the FMM regions then will be smaller, leading to a potentially larger coercive field. [8] Looking at the SQUID magnetometer data, we observe an increase in the LPCMO thin films coercive fields before and after photolithography. In Fig. 5(a), the M-H loop shows an increase of 61 Oe in the H_c at 10K after photolithography. We then measured the M-H loop at 40K, where the H_c shows an increase of 29 Oe after photolithography, as shown in Fig. 5(b). At 50K, the M-H loop in Fig. 5(c) shows a decrease of 24 Oe in the H_c after photolithography. Also at 60K, the M-H loop in Fig. 5(d) shows an increase of 2 Oe in the H_c after photolithography. These results confirm the hypothesized behavior as the increase of the coercive field after photolithography agrees with the concept of FMM regions dipole moments being smaller and more separated.

Fig. 5(e) shows the coercive field as a function of temperature for the LPCMO thin film before and after lithography. The behavior of the coercive field can be related to the phase domains of the LPCMO thin film. At 10K, the coercive field is highest due to a reduction of thermal energy attributed to the FMM regions freezing into a static state. [8] At 40-50K, the material transitions from multi-domain FMM regions to a single domain due to energy rising with the temperature. Going from small multi-domain regions to a large single-domain region increases the coercive field slightly due to the size of the single domain. Further heating decreases the size of the single FMM region decreasing the coercive field rapidly. Moving to

room temperature, the material behaves like a paramagnet with no coercive field. Comparing the coercive fields before and after photolithography over a range of temperatures, patterning LPCMO shows enhancement of the coercive field. The magnetization of the NGO substrate was plotted as a function of the inverse temperature in Fig. 5(f). According to Curie's Law, the magnetization of a paramagnetic material is inversely related to the temperature. Therefore by plotting magnetization of the NGO substrate against the inverse temperature, the result should be linear if the material is paramagnetic. Fig. 5(f) confirms our NGO substrate is a paramagnet.

The liftoff process was a novel step for our research; therefore work was done to optimize the procedure. Using the image reversal bake and flood exposure to achieve a negative image with the necessary undercut sidewalls, we were able to successfully pattern the photoresist for liftoff. Fig. 4(b) shows the areas of the contact array that ideally have no photoresist. This is where the contact with the LPCMO thin film is made. The sputter deposition of gold followed by liftoff resulted in a partial pattern transfer as seen in Fig. 4(c). This indicates photoresist or developer residue left after the photolithography. Using the AFM's optical microscope, Fig. 4(d) shows the patchy contact strips, confirming the residues effect on the liftoff. This part of the process must be optimized to see a full pattern transfer. Using the AFM's tapping mode, Fig. 4(e) shows the step from the NGO substrate to one of the LPCMO squares. From the AFM scans data, the thickness of the LPCMO thin film was determined to be 23nm.

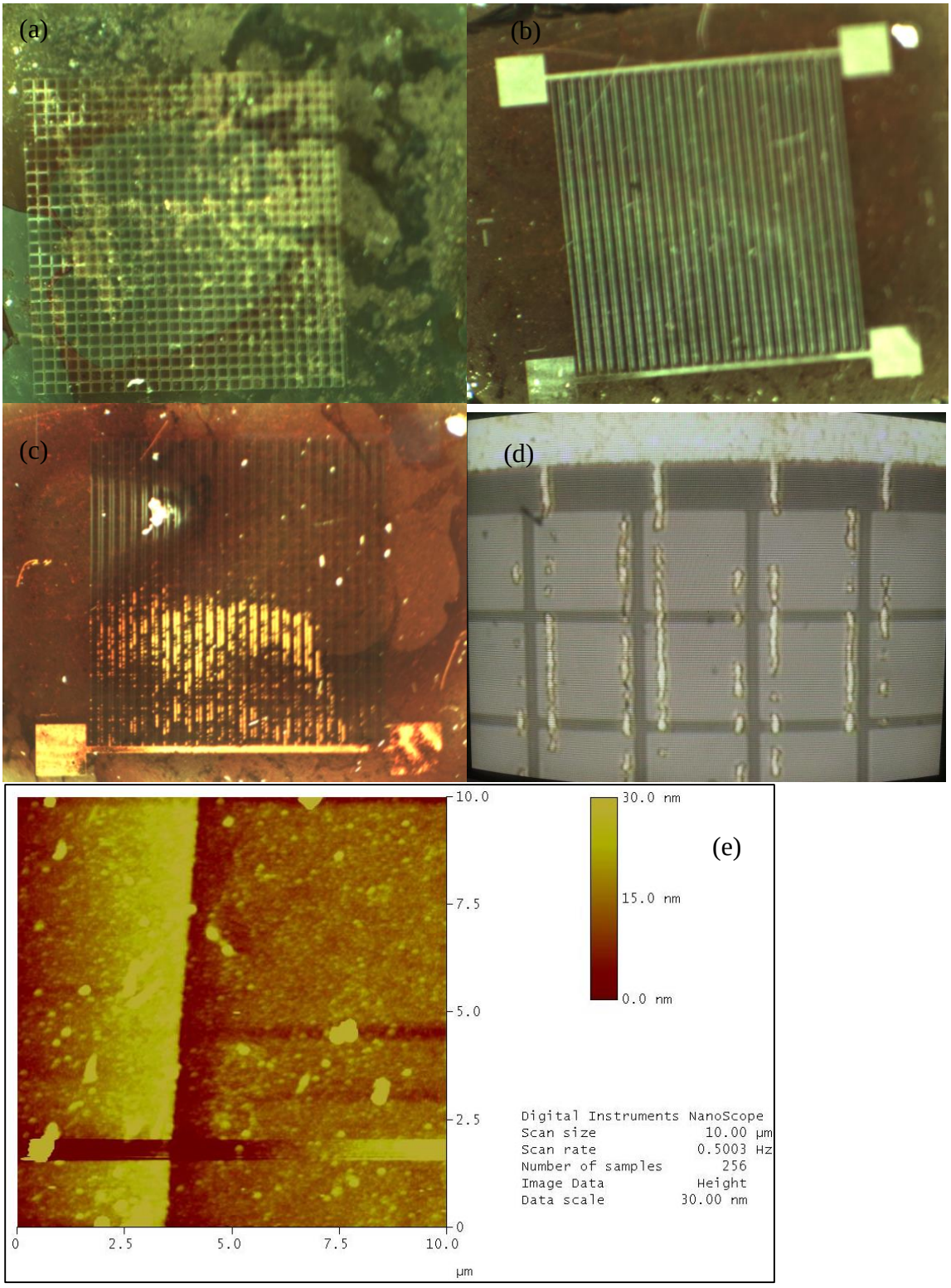

Figure 4: (a) LPCMO etch back step that forms the 27 x 27 array of 100µm squares. (b) Pattern photoresist following the image reversal process. The inset pattern represents where the gold contacts will lie. (c) Partial pattern transfer of the gold contacts following liftoff. (d) A closer view of the failed gold contact liftoff step. (e) AFM image of the step between the NGO substrate and a LPCMO square.

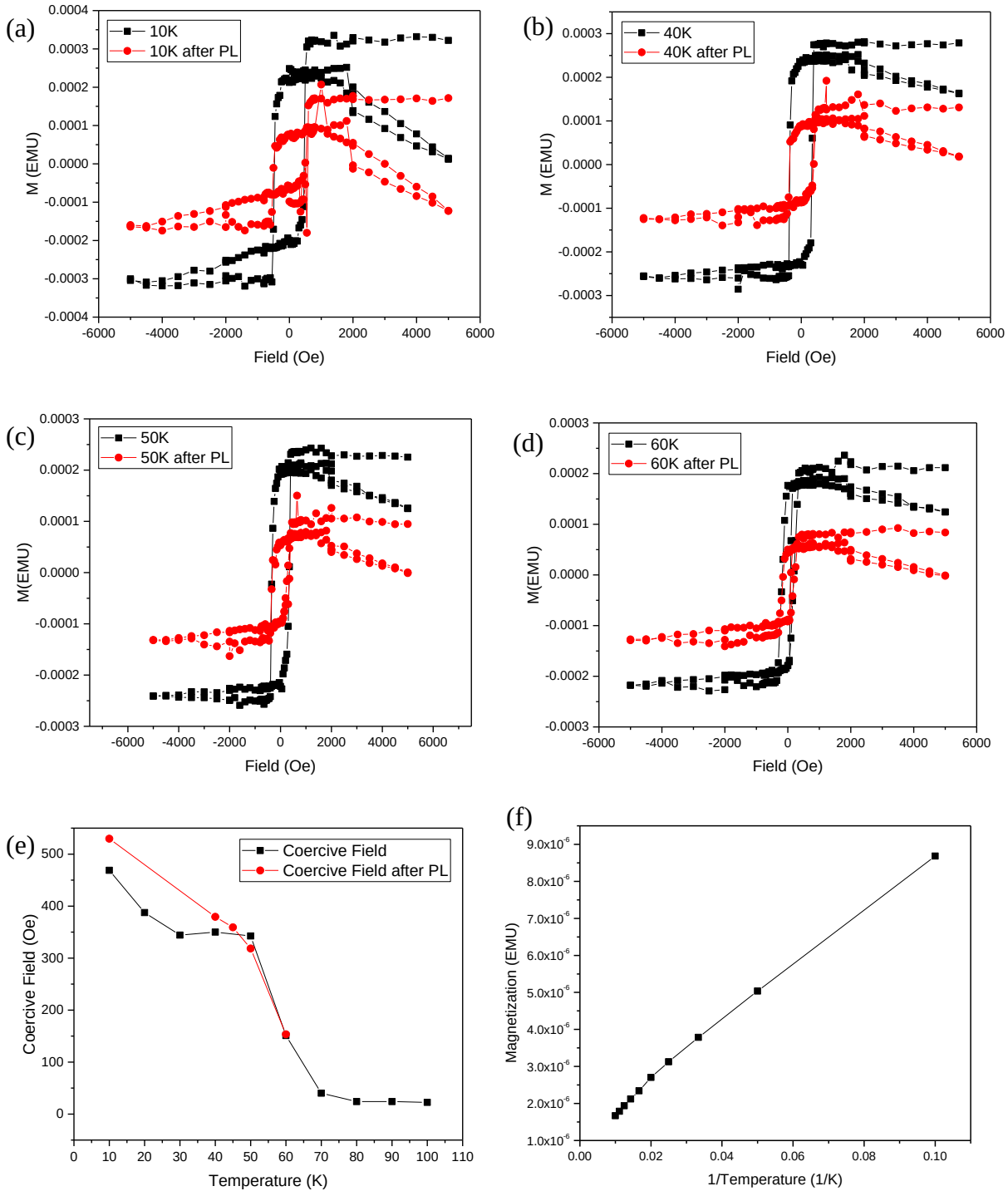

Figure 5: (a) M-H loop performed in the SQUID magnetometer at 10K. Compares the magnetization of LPCMO before and after photolithography. (b) M-H loop at 40K. (c) M-H loop at 50K. (d) M-H loop at 60K. (e) Variation of the coercive field with temperature. (f) The background subtracted paramagnetic field of the NGO substrate.

IV. Conclusions and Future Work

Gold microstructured contacts form an electrical connection with the LCPMO similar to that of the Indium soldered pads. The gold thin film as a contact array allows an external electric field to microstructured LPCMO patterns. This allows for further investigation of the effects microstructuring has on the behavior of LPCMO thin films. With a 23nm thick film of LCPMO we observed an increase of the coercive field at low temperatures after photolithography. This change showed that by isolating LPCMO regions, the coercive field was enhanced. The microstructuring of a gold contact array yielded a partial pattern transfer meaning future work will attempt to optimize this procedure. With the contact array in place, further research will be done to study the effects the electric field has on the magnetism of microstructured LPCMO.

Acknowledgements

This work was supported by NSF DMR-1461019.

Works Cited

[1] T. Dhakal, J. Tosado and A. Biswas, "Effect of strain and electric field on the electronic soft matter in manganite thin films," *American Physical Society,* vol. 75, no. 9, 2007.

[2] S. Jin, T. Tiefel, M. McCormack, R. Fastnacht, R. Ramesh and L. Chen, "Thousandfold Change in Resistivity in Magnetoresistive La-Ca-Mn-O Films," *Science,* vol. 264, 1994.

[3] S. Dong, H. Zhu and J. Liu, " Dielectrophoresis model for the colossal electroresistance of phase-separated manganites," *American Physical Society,* vol. 76, no. 13, 2007.

[4] H. Yi, T. Choi and S. Cheong, "Reversible colossal resistance switching in (La,Pr,Ca)MnO3: Cryogenic nonvolatile memories," *Applied Physics Letters,* vol. 95, 2009.

[5] A. Goyal, M. Rajeswari, R. Shreekala, S. Lofland, S. Bhagat, T. Boettcher, C. Kwon, R. Ramesh and T. Venkatesan, "Material characteristics of perovskite manganese oxide thin films for bolometric applications," *Applied Physics Letters,* vol. 71, 1997.

[6] E. Dagotto, T. Hotta and A. Moreo, "Colossal magnetoresistant materials: the key role of phase separation," *ScienceDirect,* vol. 344, no. 1-3, 2001.

[7] H. Jeen and A. Biswas, "Single domain to multidomain transition due to in-plane magnetic anisotropy in phase-separated," vol. B 83, 2011.

[8] D. M. Grant, "EFFECT OF ELECTRIC FIELD AND STRAIN ON THE MAGNETIC PROPERTIES OF PHASE SEPARATED MANGANITES," vol. Ph.D. Thesis, 2015.